ASTRONOMY & ASTROPHYSICS
SUPPLEMENT SERIES

Astron. Astrophys. Suppl. Ser. **128,** 409-416 (1998)

Wavelength calibration at moderately high resolution⋆

J.–P. De Cuyper and H. Hensberge

Royal Observatory of Belgium, Ringlaan 3, B–1180 Brussel, Belgium

Received January 24; accepted July 11, 1997

Abstract. Th–Ar lamps are commonly used as wavelength calibration units at moderately high spectral resolutions because of the richness of the Th spectrum in the visual. The inclusion of blended lines whose position is assumed to coincide with the laboratory wavelength of the principal component is shown to result in a calibration precision significantly worse than the intrinsic random noise limit. In order to avoid this degradation of the calibration, we present resolution–dependent Th–Ar wavelengths in the region 277 to $>$ 1 000 nm for use at pixel–scales between $\lambda/2.5\,10^4$ and $\lambda/10^5$.

Key words: methods: data analysis; techniques: spectroscopic

1. Purpose

The purpose of this paper is to provide input data for Th–Ar wavelength calibration lamps that allow to approach the random noise limited centering accuracy on individual calibration lines. The rich Th spectrum produces many blended features at moderate resolutions. The majority of the lines is unblended only at pixel–scales $> \lambda/10^5$. Even when a blending line is weak compared to the intensity of the principal component, its influence on centering algorithms is shown to exceed often by far the uncertainty due to random noise. We produce a table of calibration lines for different moderate resolutions, from which the user can easily extract a line list with resolution–dependent blend wavelengths. In this way, the user keeps the freedom to apply the selection at a level of rigidity compatible with his goals and the specific format of the observations. The tables encompass the range in pixel–scale from a lower limit $\lambda/2.5\,10^4$ below which so many Th lines are badly blended that another lamp should be used for accurate calibration, up to an upper limit $\lambda/10^5$ above which blending is a minor problem (selecting all completely unblended lines at $\lambda/10^5$ already gives ample calibrator lines).

The application that profits most from the use of a list of line positions with high individual accuracy is the derivation of an adequate analytical calibration relation $\lambda = \lambda(x_1, x_2)$ where x_1 and x_2 refer to the position on the detector. Usually x_1 is along the detector rows or columns, whichever is approximately parallel to the spectral orders, and x_2 varies with the number of the spectral order or along the slit. Accurate input data allow to derive a more robust relation (Hensberge & Verschueren 1989), rather than using (bivariate) polynomial approximations, that, especially in the case of multi–order (echelle) registrations, induce many uncoupled parameters without physical meaning.

The availability of few–parameter accurate fit relations will further gain importance with the use of arrays of CCD's in spectroscopy. Indeed, one echelle order may then be projected in parts on different detectors which will never be perfectly aligned. With this orientation problem entering the calibration procedure, an inclusion of unnecessary degrees of freedom would induce still more instability.

In Sect. 2, general arguments on the attainable precision and on line blending effects are summarized. The method used to determine the corrected blend wavelengths is presented in Sect. 3. A short statistical discussion of the results is given in Sect. 4. The availability and the applicability of the selection tables are described in Sect. 5. In Sect. 6 we briefly discuss to what extent the line selection requires the use of robust, few–parameter calibration relations, and comment on the risks involved in some common alternative approaches.

2. Centering accuracy

2.1. Precision of line positions

In the absence of systematic errors, the centering accuracy on wavelength calibration lines is random noise

Send offprint requests to: J.-P. De Cuyper, Jean-Pierre.DeCuyper@oma.be

⋆ Full Tables 5 and 6 are only available in electronic form at the CDS via anonymous ftp to cdsarc.u-strasbg.fr (130.79.128.5) or via http://cdsweb.u-strasbg.fr/Abstract.html

limited. Brown (1990) derived that the photon–noise limited accuracy of centering may be estimated as:

$$\frac{1}{V_c} = \sum_i \frac{1}{I_i} \left(\frac{\mathrm{d}\, I_i}{\mathrm{d}\, \lambda} \right)^2 \quad (1)$$

where V_c is the variance on the position of the line centre in wavelength squared units, I_i is the observed intensity at pixel i and the sum extends over the window used for centering. The lines are assumed sufficiently strong to make read–out noise negligible; the generalisation to faint lines is however straightforward.

A useful estimate of $V_c\,[\mathrm{pix}^2]$ is obtained using a Gaussian line profile and neglecting (for simplicity) discretisation and edge effects, integrating over an infinite interval rather than summing over a finite one gives:

$$V_c = 0.17\, \frac{FWHM}{I_c}. \quad (2)$$

Many lines are usually available with $I_c \gg 10^3$ detected electrons on their central pixel. In the case of critically sampled lines (full-width at half maximum $FWHM < 2$ pix), the photon–noise limit is thus close to 0.002 pix ($I_c = 10^5$), 0.006 pix ($I_c = 10^4$) or 0.018 pix ($I_c = 10^3$) depending on the line strength. Hence a positional accuracy on individual calibration lines of the order of 10^{-2} pix is *in principle* attainable. This conclusion remains valid after taking into account the model–mismatch errors discussed by David & Verschueren (1995), when the proper precautions are made.

In practice, however, the residuals of the lines to a best fit are significantly larger. This is mainly due to the fact that laboratory input data are used at face value, without concern for the effects of line blending at the actual resolution of the astrophysical instrument.

2.2. Line blending at moderate resolution

Intuitively, it appears that the adverse influence of blending may be eliminated by rejecting the outlying residuals through a clipping algorithm. Hensberge & Verschueren (1990) showed for Th, why clipping algorithms are rather inefficient: the distribution of the centering bias due to blending is monotonously decreasing rather than multimodal, and the larger part of the distribution extends to biases largely exceeding the random noise. Hence, a clipping algorithm only eliminates the most obviously blended lines. One should keep in mind that apparently weak blends, not easily noticeable on an individual measure with the instrument's optimal S/N, can still produce systematic centering errors which are an order of magnitude above the noise limit (see De Cuyper & Hensberge 1995). A stringent selection of useful lines is needed for critical applications: the residuals of a fit to the measured line positions will be useful for testing the suitability of the fit formula only when the rms induced by blending is negligible with respect to the contribution of random noise.

3. Method

Table 1 summarizes the parameter combinations used in the computations. The five moderately high resolutions considered here are described by their pixel–scale, defined as the pixel–size expressed in wavelength units. The lines are assumed to have Gaussian profiles. The critical assumption is the symmetry of the lines, the exact shape has less importance. Their width is representative for critically sampled Th–Ar lines obtained with several moderate dispersion spectrographs (e.g. ARC at Yerkes, BME at CTIO, CASPEC at ESO, ELODIE at OHP, ESPRESSO at SPM, UCLES at AAO, UES at La Palma, ...).

Table 1. Characteristics of the degraded laboratory spectra and the fitting process. The Ar line intensities in the last two rows refer to the "standard" and to the "Ar rich" case (line positions in Å)

quantity	specification(s)
λ/pixel–scale	100 000, 50 000, 43 700, 33 333, 25 000
Line shape	Gaussian
Line width	$\sigma = 0.8$ pix
Fit function	$a_0 + a_1 \exp -\frac{(x-c)^2}{2\,\sigma^2}$
Fit interval	7 pix
Ar I intens.	$I_{\mathrm{Ar\,I}\ \lambda\,4300.1}/I_{\mathrm{Th\,I}\ \lambda\,4313.0} = 1.267$ or 28.68
Ar II intens.	$I_{\mathrm{Ar\,II}\ \lambda\,4309.2}/I_{\mathrm{Th\,I}\ \lambda\,4307.2} = 1.922$ or 43.48

Table 2. Sources of laboratory data

reference	element, ion
Minnhagen[1] (1973)	Ar I
Norlén (1973)	Ar I & Ar II
Palmer & Engleman (1983)	Th I & Th II

[1] We scaled the sources for Ar I to each other by $S_{\mathrm{Norlén}} = S_{\mathrm{Minnhagen}}/\,(1.2 + 0.02\, S_{\mathrm{Minnhagen}})$ where S is the author's intensity parameter in a log scale with base $\sqrt{2}$.

The relative intensities of the lines are taken from the laboratory sources mentioned in Table 2. The Ar intensities are scaled against the Th intensities in two different ways (Table 1). The applied ratios correspond to the output of the Th hollow cathode lamps provided by S&J Juniper (CAT NO 4160QA) with an Ar gas fill pressure of 5 mB and a quartz window, operated "standard" at $\approx$ 10 mA, but the "Ar rich" spectra have been obtained presumably at a higher, but not exactly known, lamp current. The main purpose of analyzing the blending in these two different cases is to gain insight in how far this scaling might invalidate the selection of useful calibrators. The output of Th–Ar lamps used with other spectrographs differs, as far as we could check, much less from one of

these cases than the factor $16\sqrt{2}$ which separates the here adopted Ar–to–Th ratios, although not all lie in between these two cases. It should be noted that the result for most blends does not depend on this scaling: it turns out that at least 80% of the *useful* lines (and much more at smaller pixel–scales) is not or not significantly affected by a large change in the Ar–to–Th intensity ratio. Moreover we indicate in Sect. 5 several ways to detect or remove lines that would have been inappropriately selected as useful because of bad assumptions in the ratios of the blending components.

Anyway, the use of preset intensities is a drawback in predicting the effective blend wavelengths; even Th–Th blends might be affected by the operating lamp current and aging effects. It cannot be the purpose of such computations to predict large corrections precisely for any lamp, and surely not for different lamps. In view of the need for general usefulness of the final calibrator lists, one is therefore obliged to include in these lists only blends with corrected positions deviating from the laboratory wavelength of the stronger component by less than twice the rms due to random noise. Hence, lines that were found to have a displacement $|\delta p| > 0.05$ pix due to blending have been eliminated in an early stage of our two–step calculation method.

In the first step, a grid of synthetic spectra consisting of two Gaussians separated by a distance d, $0.1 \text{ pix} \leq d \leq 6$ pix, and with $0.01 \leq I_\mathrm{b}/I_0 \leq 1.0$, is subjected to a least–squares Gaussian fitting routine to find out when displacements $|\delta p| \approx 0.05$ pix are to be expected. The subscripts b and 0 refer to the blending and the principal component. The fit function includes a (constant) background term a_0 for consistency with several software packages in use in astronomical spectroscopy. The principal Gaussian is placed exactly in the centre of the seven pixels long fit interval. The resulting grid of displacements is used to decide for each laboratory line under study whether it is with certainty intolerably blended, or whether a more detailed analysis is useful. An important reduction in computing time results: 40% and 80% of the lines are rejected based on this simple criterion, for pixel–scales of $\lambda/10^5$ and $\lambda/2.5\,10^4$ respectively. It is possible that in the case of a line blended by several others, a more detailed computation would give a displacement slightly below 0.05 pix, since blending lines on different sides of the principal component can cancel partly the adverse effect of each other. Tests indicate that this occurs rarely ($\ll 1\%$ probability); and even then, the result is very sensitive to the sub–pixel location of the centre of the line and thus a discretisation–independent predicted displacement would remain inaccurate (see the discussion of the second step for an evaluation of discretisation-dependent effects).

Figure 1 clarifies what kind of blends are marked as intolerable. A blending line with an intensity of only 10% of the intensity of the principal component can produce a displacement $|\delta p| > 0.05$ pix when it is situated at a distance of $0.6 \leq d \leq 2$ pix. Stronger blending lines produce shifts in the order of tenth(s) of a pixel over a wide range in separation.

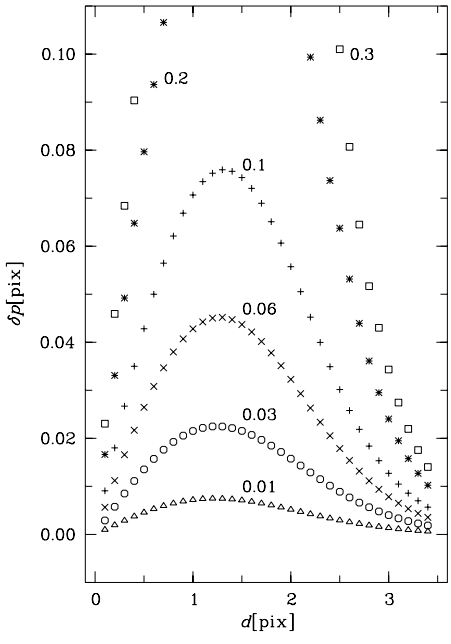

Fig. 1. Displacement δp of the line centre due to one single blending component at a distance d. The curves are labelled with their corresponding relative intensity I_b/I_0

If in the first–step estimation the predicted displacement $|\delta p| < 0.05$ pix, then the line is subjected to a more stringent test in a second step, or, if the line is found to be quasi–isolated, then its laboratory position is marked as unaltered. Quasi–isolation was defined by:

$$d \geq \left[4.5 + \log\left(\frac{2I_\mathrm{b}}{I_0}\right)\right] \text{ pix} \qquad (3)$$

for all blending components. This corresponds to a (neglected) displacement $|\delta p| < 0.005$ pix. The intensity of the blending components was arbitrarily enhanced by a factor 2 over the intensity I_b given in the laboratory source to account for the case of blending with several lines near to each other that have similar intensities. In this step the only requirement is to label no line errorneously as quasi–isolated, while the number of missed quasi–isolated lines should remain small relative to the total number of lines that need a further check. The fraction of quasi–isolated lines detected in this way varied from 40% at a pixel–scale of $\lambda/10^5$ to only 5% at $\lambda/2.5\,10^4$. Hence, after the elimination of the intolerably blended lines and the quasi-isolated ones in this first step, there remain only $15-20\%$ of the lines for further testing irrespective of the pixel–scale considered.

In the second step, the spectrum around the considered laboratory line is calculated for a full grid of sub–pixel

locations of the line centre, as the Gaussian fit depends on discretisation because of model–mismatch (David & Verschueren 1995). The line centre was shifted in steps of 0.05 pix (until the same discretisation repeated after 20 steps) and the Gaussian fit was explicitly made for each case. The average position of the fitted Gaussian line centre over these twenty trials defines the effective wavelength of the blended laboratory line for a given pixel–scale. In the case of complicated blends, the result may be too sensitive to discretisation and the average would become meaningless. The same may occur when the wing of a strong blending line affects the intensity at the edge of the fit interval. Such cases are marked as unsuitable for calibration purposes, like the ones eliminated in the first computational step. The rejection criterion used is that $s > 0.015$ pix, where s is the rms of the fitted line centre computed from the twenty discretisation trials.

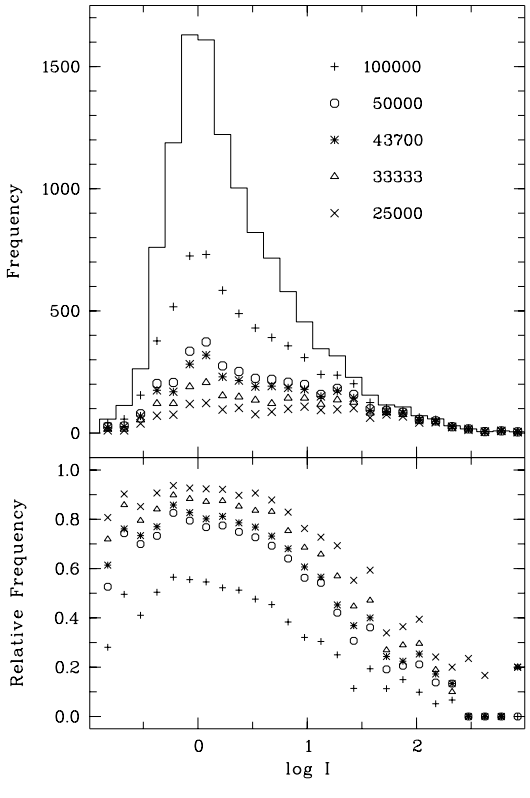

Fig. 2. Number of selected lines in bins of relative line strength, for different pixel–scales (labels refer to λ/pixel–scale). The full line is the input distribution (laboratory resolution). The lower panel gives the fraction of rejected lines in the same parameter space

The complications discussed here imply that the decision on usefulness depends for a minority of lines critically on the fit interval used. A seven pixel interval corresponds in our sampling case to 3.7 FWHM. There is no reason to consider in a rich spectrum a larger interval, since in the absence of blending effects at the edges, the background is well sampled. A smaller interval is less vulnerable to wide blends, but more to overfitting of closer blends, to errors in background estimation and to systematics with sub–pixel location (in the case of our 4–parameter fit). However, the fit function used might be constrained better using a priori information: background subtraction is in principle easy and the FWHM of the PSF could be constrained to vary at most slowly over the whole frame. At present, we only state that improvements in this sense might be considered, but are not applied in the commonly used software packages. The computation with the seven pixel interval is safe in the sense that it rejects too many lines (for a given line width), rather than provide the user with a selection containing some potentially bad calibration lines.

4. Statistical analysis

The upper panel of Fig. 2 shows the distribution of the selected lines at different pixel–scales (different symbols) versus relative line strength (abscissa). The lower panel displays the information alternatively as the fraction of rejected lines at a given pixel–scale and line intensity. One should keep in mind that the lines useful for calibration purposes are in the longward intensity tail, roughly at $\log I > 0.5$. The fraction of rejected lines depends strongly on the pixel–scale. At lower pixel–scales (higher resolutions) than considered in this paper, enough totally unblended lines can be selected. At higher pixel–scales (lower resolutions) than considered here, almost all Th lines are blended. The absolute number of useful lines does not increase significantly towards lower line intensities. This is true over almost the whole pixel–scale interval under consideration. Hence, the use of more (and thus also weaker) lines without appropriate selection for blends, in an attempt to average out most of the blending influences, inevitably introduces more strongly blended lines with lower S/N! The conclusions presented here remain valid for more restricted wavelength intervals within our considered range.

From here on, we restrict our attention to the subsample of useful lines. Figure 3 shows the distribution of the selected lines over wavelength, together with the input distribution. At the higher pixel–scales, the absolute number of useful lines in the red becomes higher than in the blue, while the original input data show a line density ratio of roughly 3 in the other sense. The crowding of lines in the blue Th spectrum starts to provide more useful calibrators than in the red only at pixel–scales $< \lambda/6\,10^4$.

The distribution of the displacements of the selected calibration lines is shown in Table 3 for the different pixel–scales. The strong concentration towards low values indicates that the number of useful lines does not increase

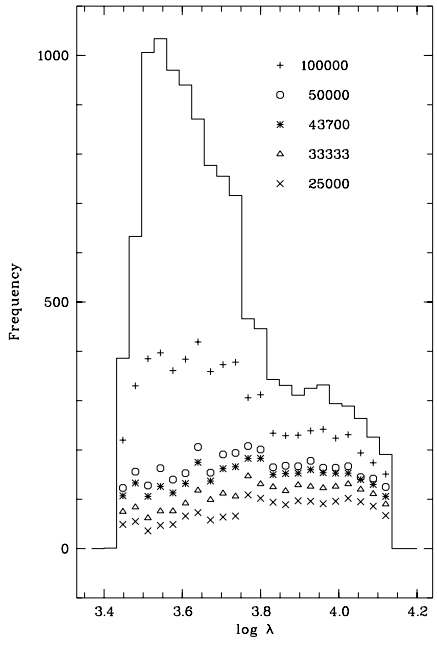

Fig. 3. Distribution in wavelength (log–bins) of the original sample and of the samples selected at the different pixel–scales. Symbols as in Fig. 2

significantly by including lines with displacements larger than a few 10^{-2} pix.

Table 3. The number of selected lines with a displacement δp from the position of the principal component inside the range given in the first column for different pixel–scales (column headers refer to λ/pixel–scale)

$\lvert\delta p\rvert$ [pix]	100 000	50 000	43 700	33 333	25 000
< 0.005	2069	1209	1051	771	523
0.005–0.010	105	136	121	110	127
0.010–0.020	145	162	195	175	152
0.020–0.030	89	105	111	129	109
0.030–0.040	72	84	76	78	62
0.040–0.050	44	40	40	41	40

The stability of the predicted blend wavelength with respect to sub–pixel location is in the large majority of the selected cases excellent with respect to the required accuracy (Table 4). The correlation between displacement $|\delta p|$ and discretisation stability s is shown in Fig. 4. Also these data suggest that a selection on the stability indicator that is stricter than the one used in the calculations ($s \leq 0.015$ pix) is appropriate. We suggest to use $s < 0.0025-0.005$ pix depending on the pixel–scale.

Table 4. Discretisation stability of the blend wavelengths of the selected lines for a given pixel–scale (column headers refer to λ/pixel–scale). The parameter s given in the first column, is the rms of the blend wavelengths calculated for 20 different discretisations in steps of 0.05 pix

s [pix]	100 000	50 000	43 700	33 333	25 000
< 0.001	2252	1448	1310	1019	740
0.001–0.003	163	166	149	168	146
0.003–0.005	66	65	80	64	65
0.005–0.010	35	34	34	30	41
0.010–0.015	8	19	18	17	19

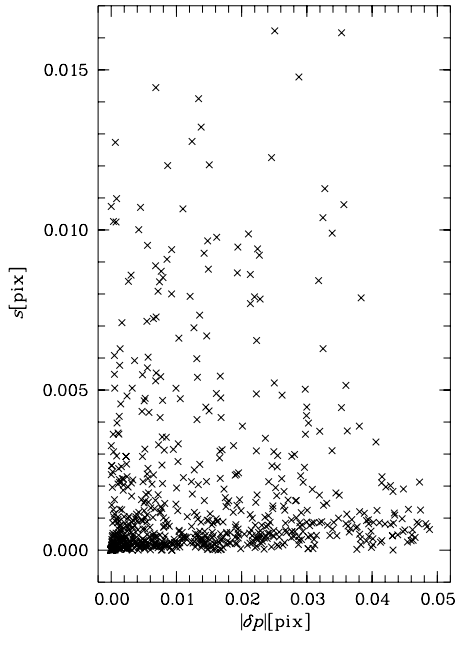

Fig. 4. Line displacement $|\delta p|$ against discretisation stability s (see also Tables 3 and 4) for the highest pixel–scale $\lambda/2.5\,10^4$. Only lines with $d \leq 0.05$ pix and $\log I > 0.5$ are shown. At lower pixel–scales, the data occupy the same area, but with an increasing density towards small displacements and high stability

5. Improved Th and Ar input wavelengths

The improved Th and Ar input wavelengths for moderately high resolutions in astronomy are given in the electronic appendix of this paper, as ASCII tables. A sample page of the principal table is shown in Table 5. In addition to the original laboratory wavelength and the resolution–dependent improved blend wavelengths, it contains additional information giving the user freedom in the choice of his selection limits. However, no corrections are given for heavily blended lines, as such corrections are intrinsically uncertain. Restricted tables, listing only the resolution–dependent blend wavelength of preselected lines together

Table 5. Sample page of the principal table for the "standard" case of the Ar–to–Th line strength ratio (see Table 1), showing the laboratory wavelength [Å] (Col. 1), the emitting ion (Col. 2) and the relative intensity in log–scale (Col. 3) of the principal component; the resolution–dependent blend wavelengths [Å] (Cols. 5–9), and their corresponding displacement δp [pix] and discretisation stability parameter s [pix] (Cols. 10–20). The headers of Cols. 5–9 refer to λ/pixel–scale and the headers of Cols. 10–20 refer to $10^{-3}\,\lambda$/pixel–scale

maincomp	ion	logint	lam025000	lam033333	lam043700	lam050000	lam100000	dp025	s025	dp033	s033	dp043	s043	dp050	s050	dp100	s100
4703.9898	Th I	2.16	4703.9891	4703.9895	4703.9895	4703.9895	4703.9895	−0.004	0.000	−0.002	0.000	−0.003	0.000	−0.003	0.000	−0.006	0.000
4704.4975	Th	−0.34															
4704.6560	Th II	−0.23															
4705.2986	Th II	−0.19					4705.2986									0.000	0.000
4705.6175	Th II	0.45															
4705.7606	Th II	1.24					4705.7596									−0.021	0.001
4706.2511	Th II	0.50					4706.2511									0.000	0.000
4706.5771	Th I	0.18					4706.5771									0.000	0.000
4707.0450	Th	0.11			4707.0443	4707.0449	4707.0450					−0.006	0.002	−0.001	0.000	0.000	0.000
4707.7734	Th I	−0.28					4707.7734									0.000	0.000
4708.1004	Th II	0.10															
4708.2940	Th I	1.10					4708.2939									−0.001	0.000
4710.8238	Ar II	0.00															
4710.9921	Th	0.18					4710.9909									−0.026	0.005
4711.4184	Th I	0.32			4711.4177	4711.4182	4711.4184					−0.006	0.008	−0.002	0.001	0.000	0.000
4712.0056	Th I	0.32					4712.0056									0.000	0.000
4712.3921	Th II	0.33															
4712.4814	Th I	1.39															
4712.8408	Th I	0.88					4712.8414									0.013	0.001
4712.9684	Th	−0.34															
4713.7914	Th I	−0.23		4713.7914	4713.7914	4713.7914	4713.7914		0.000	0.000		0.000	0.000	0.000	0.000	0.000	0.000
4714.6715	Th I	0.22		4714.6715	4714.6715	4714.6715	4714.6715		0.000	0.001		0.000	0.000	0.000	0.000	0.000	0.000
4715.4308	Th II	0.42		4715.4307	4715.4308	4715.4308	4715.4308		−0.001	0.003		0.000	0.000	0.000	0.000	0.000	0.000
4716.0618	Th I	0.07		4716.0606	4716.0618	4716.0618	4716.0618		−0.009	0.003		0.000	0.000	0.000	0.000	0.000	0.000
4717.3905	Th I	−0.03		4717.3903	4717.3905	4717.3905	4717.3905		−0.001	0.005		0.000	0.000	0.000	0.000	0.000	0.000
4718.0554	Th I	−0.06				4718.0552	4718.0554							−0.002	0.007	0.000	0.000

with the laboratory wavelength and the emitting ion of the principal component, are also available; a sample page is given in Table 6. Lines that are in principle useful but intrinsically weak, and mixed Th–Ar blends giving results too dependent on the relative strength of the Ar versus Th components were removed from these ready–to–use lists.

Table 6. Sample page of the restricted table for pixel–scale $\lambda/43700$, giving the blend wavelength [Å] (Col. 1), the laboratory wavelength (Col. 2) and the emitting ion (Col. 3) of the principal component

λ blend	maincomp	ion
4686.1946	4686.1946	Th I
4690.6235	4690.6219	Th I
4694.0914	4694.0914	Th II
4698.2248	4698.2248	Th
4703.9895	4703.9898	Th I
4726.8683	4726.8683	Ar II
4732.0543	4732.0532	Ar II
4735.9064	4735.9058	Ar II
4739.6784	4739.6764	Th I

Considerations that might influence the user's selection choice are e.g.

- the calibration accuracy of interest for the specific problem; as a rule of thumb, no lines should be included with a computed displacement exceeding the aimed *local* wavelength accuracy, and intrinsically useful but too noisy lines should not be used (user defined S/N cut-off of faint lines).
- the change of detector sensitivity with wavelength and through one spectral order. An even distribution of the calibrator lines over the frame is the best guarantee for an optimal local accuracy. Nowhere lower quality data should degrade nearby high quality data (locally defined S/N cut-off). As this aspect of the selection depends very specifically on the observing conditions, it must necessarily be the concern of the user if one wants to obtain the highest possible accuracy.
- the difference between the centering algorithm used and the one applied in our calculations. The sensitivity of centering methods to asymmetry depends on the algorithm, and hence the measured blend wavelength depends on the algorithm. (e.g. the centre of gravity is much more sensitive than a gaussian fit to the asymmetries at the edges of the fit interval.) The use of a

different fit interval will change the predicted wavelengths for those few cases where a strongly blending line (or line wing) is near the edge of the interval.
- the difference in observed and assumed line width. Broader calibration lines lead to an increase of bias in the wider blends. For the weak blends of interest here, significant differences in predicted position may occur for blends composed of components separated by more than two pixels if the PSF is at least 25% broader than assumed in our computations. Thus, differences in line width or in centering algorithm both require a more stringent selection of the wider blends.
- the observed Ar–to–Th line strength ratio. The fact that the principal table contains results for two different Ar–to–Th line strengths and the relative strengths of all lines (for comparison with ones observations) permits to evaluate the risk of using specific mixed blends. Note that the fraction of potentially useful Th–Ar features sensitive to the Ar–to–Th ratio is small (Sect. 3); a "fast and safe" solution is to disregard them always.

The user can make a final check on the selection and line centering procedure for a particular lamp spectrum by inspecting the residuals between the measured line positions and the ones predicted by his calibration model (assuming the latter model is precise). The residuals for a given line on different frames should not correlate with discretisation (i.e., with the sub–pixel position of the line centre), and its average value over all frames should not deviate significantly from 0. A correlation with discretisation for completely unblended lines indicates that the line centering procedure contains (implicit) invalid assumptions about the PSF. This may also lead to an offset from 0 when not all discretisations are evenly sampled in the set of frames. Blended lines are expected to give rise to residuals that correlate with discretisation to the extent described by the parameter s in our tables. Significant offsets from 0 may hint to biased theoretical wavelengths. Such outliers, if any, should be rare (as argued in Sect. 3) after application of the proposed "cleaned" calibrator lists and thus easily recognizable.

6. Discussion

Th calibration lamp spectra are commonly used at resolutions at which line blending displaces the majority of the measured features from the laboratory wavelength of their principal component by an amount which is large compared to the random noise limited centering accuracy. Earlier, we derived improved wavelengths in a restricted wavelength and resolution domain and obtained through their use more accurate wavelength calibrations. Here we derive improved resolution–dependent wavelengths for the full subset of at most weakly blended Th and Ar features in the whole wavelength and resolution domain of interest. This work should encourage the search for more robust wavelength calibration techniques.

The use of higher order polynomial approximations in wavelength calibrations should be discouraged. First, proper care should be given to the elimination of systematic effects that dominate over random noise. Otherwise, the higher order terms will be determined by the trend in the systematic effects towards the ends of the wavelength range; as a consequence, and in spite of the lower internal scatter with respect to the calibration line positions, the model is then likely to deviate further from reality than a low order polynomial. In fact, the use of appropriate wavelengths strongly enhances the power to discern significant terms from spurious ones.

The elimination of the calibration bias due to blended lines leads to a better accuracy, even while using less numerous calibration points. When the calibration relation itself depends on a low number of fit parameters, then the full advantage of the higher accuracy of the input data can be conserved. Unfortunately, in echelle spectroscopy the practice of fitting a polynomial approximation to each order independently is still common. This leads to many parameters to be determined, i.e. $m.n$ for a $(m-1)$th degree approximation on n orders, which is usually of the order of 10^2! In general, such approach will prevent to make the proper line selection (our experience at λ/pixel–scale of 3 to $4\,10^4$ gave densities of selected lines of 7 per spectral order on the average, but some orders had very few lines). This is however not a fundamental problem, as we could reduce the number of free parameters by more than a factor 10 once we took care of the blending effects by deriving an adequate 7-parameter 2–D relation (Hensberge & Verschueren 1989).

The argument that the use of much more, partly fainter and stronger blended lines would lead to a comparable final calibration accuracy, because the blending effects will statistically largely cancel, appears wrong: first of all, the total number of quasi–unblended weak lines does not increase sufficiently fast with decreasing intensity in order to compensate for the larger random errors on individual lines. Secondly, even when numerous blended lines are included, the line density is insufficient to smooth away significant chance fluctuations in the distribution of the line displacements: large calibration errors at particular locations are to be expected, while the global calibration accuracy might be appropriate for many purposes.

Once the accuracy of the calibration is limited mainly by random errors, further gains can be expected from coupling the calibration from different frames (see Verschueren et al. 1997). This aspect is still under investigation and falls beyond the scope of the current paper.

Appendix A: Tables in electronic form

A principal table containing five resolution–dependent blend wavelengths together with their corresponding pixel displacement δp and discretisation stability parameter s for two very different Ar–to–Th line strength ratios, as

well as five restricted tables containing only the blend wavelengths of a selection of strong stable calibration lines for each of the spectral resolutions discussed in this paper are published by A&A at the Centre de Données de Strasbourg, where they are available in electronic form: see the Editorial in A&A 1993, Vol. 280, page E1. These tables are also available on the webserver of the Astrophysics Data Reduction Centre of the KSB/ORB: http://midas.oma.be or through anonymous ftp from midas.oma.be.

Acknowledgements. Both authors carried out the research in the framework of projects initiated and financed by the *Belgian Federal Scientific Services (DWTC/SSTC)*, contract *Service Centres and Research Networks* No. SC/005 and contract *I.U.A.P.* No. P4/05. They are grateful to M. David and W. Verschueren for discussions and a critical reading of the manuscript.

References

Brown T.M., 1990, in CCD's in Astronomy, Jacoby G.H. (ed.) p. 335

David M., Verschueren W., 1995, A&AS 111, 183

De Cuyper J.–P., Hensberge H., 1995, in ADASS IV, Shaw R.A., Payne H.E. and Hayes J.J.E. (eds.) ASP Conf. Ser. 77, 476

Hensberge H., Verschueren W., 1989, The Messenger 58, 51

Hensberge H., Verschueren W., 1990, in Errors, Bias and Uncertainties in Astronomy, Murtagh F., Jaschek C. (eds.). Cambridge Univ. Press, p. 335

Minnhagen L., 1973, J. Opt. Soc. Am. 63, 1185

Norlén G., 1973, Phys. Scripta 8, 249

Palmer B.A., Engleman R. Jr., 1983, Atlas of the Thorium Spectrum, Sinoradzky H. (ed.) Los Alamos National Laboratory

Verschueren W., Brown A.G.A., Hensberge H., et al., 1997, PASP 109, 868